Vinca Alkaloid-Induced Tubulin Spiral Formation Correlates with Cytotoxicity in the Leukemic L1210 Cell Line†

Sharon Lobert,*,‡,§ Jacques Fahy,|| Bridget T. Hill,|| Alain Duflos,|| Chantal Etievant,|| and John J. Correia§

School of Nursing and Department of Biochemistry, University of Mississippi Medical Center, Jackson, Mississippi 39216 and Institut de Recherche Pierre Fabre, F81106 Castres, France

Received May 5, 2000; Revised Manuscript Received July 31, 2000

ABSTRACT: The ability of a class of C-20′ modified vinca alkaloid congeners to induce tubulin spiral formation was investigated relative to their ability to inhibit microtubule assembly, their cytotoxicity against a leukemic cell line, L1210, and their measured and calculated partition coefficients. These studies were prompted by the observation that the energetics of vinca alkaloid-induced tubulin spiral polymers, or spiraling potential, is inversely related to their clinical dosage and are aimed at the long-term goal of developing the ability to predict the cytotoxic and antineoplastic properties of antimitotic drugs. We demonstrate here that vinca-induced tubulin-spiraling potential is significantly correlated with cytotoxicity against L1210 cells. This is consistent with the size of spirals formed being proportional to the relaxation time for polymer redistribution, the lifetime of cell retention, and effects on microtubule ends and dynamics. Spiraling potential also correlates with calculated but not measured partition coefficients. Surprisingly, spiraling potential does not correlate with the ability to inhibit microtubule formation with purified tubulin or microtubule protein. For the set of C-20′ modified compounds studied, the largest inhibitory effects on spiraling potential and cytotoxicity are caused by multiple sites of halogen (-F, -Cl) substitution with the introduction of increased rigidity in the ring. This suggests the C-20′ position interacts with a hydrogen bond acceptor or an electrophilic region on the protein that electrostatically disfavors halogen substitutions. These studies are discussed in terms of the cellular mode of action of antimitotic drugs, particularly the importance of microtubule dynamics during mitosis and the factors that regulate those dynamics.

The vinca alkaloids, vinblastine,[1] vincristine, and vinorelbine, are included in many chemotherapy protocols, yet the molecular origins of their differential antitumor and toxic side effects remain uncertain. Both vincristine and vinblastine were first used in the 1960s for the treatment of Hodgkin's lymphoma. Since that time, they have been effective against a spectrum of hematologic and solid tumors (*1*). Vinorelbine is widely used for the treatment of breast cancer and nonsmall cell lung carcinoma (*2*) and most recently vinflunine, a newer fluorinated derivative, has undergone phase I clinical evaluation in Europe with phase II trials planned. Vincas in vivo interact with tubulin at the ends of microtubules in mitotic spindles and diminish dynamic instability resulting in mitotic arrest (*3*, *4*). At substoichiometric concentrations, these drugs inhibit assembly of microtubules, whereas at higher concentrations, they cause dissolution of microtubules, inducing formation of tubulin aggregates (spirals, coils, paracrystals). Drug binding is linked to spiral formation, and a Wyman linkage model best describes vinca alkaloid binding data (*5*, *6*). The overall binding affinity is the product of equilibrium constants, K_1K_2, that describes drug binding to tubulin, K_1, and drug-induced tubulin spiral formation, K_2, and will be referred to here as the spiraling potential. Spiraling potential directly reflects spiral size since K_2 is a direct measure of the affinity of liganded tubulin heterodimers for growing spiral polymers. Data collected by sedimentation velocity and fit with this model demonstrated that the order of spiraling potential, vincristine > vinblastine > vinorelbine > vinflunine (*7*, *8*), agrees well with the weekly intravenous doses used clinically, where vincristine < vinblastine < vinorelbine (*9*). This demonstrates that chemical differences in vinca alkaloids result in different drug-induced spiraling potential, and we have hypothesized that tubulin spiral formation is linked to therapeutic effects (*6*).

Vincristine differs from vinblastine at the R1 position in the vindoline moiety where a formyl group replaces a methyl group (Figure 1). Vinorelbine differs from vinblastine in its cleavamine moiety by modification at C4′ with an eight instead of a nine-membered ring and a 3′,4′ double bond. Vinflunine is a derivative of vinorelbine difluorinated at the

† This work is supported by NIH Grant NR04780 (S.L. and J.J.C.) and Institut de Recherche Pierre Fabre.

* To whom correspondence should be addressed: Dr. Sharon Lobert, University of Mississippi Medical Center, School of Nursing and Department of Biochemistry, 2500 N. State St., Jackson, MS 39216. Phone: 601-984-1852; fax: 601-984-1501; e-mail: slobert@son.umsmed.edu.

‡ School of Nursing.

§ Department of Biochemistry.

|| Institut de Recherche Pierre Fabre.

[1] Abbreviations: EGTA, [ethylene-bis(oxyethylenenitrilo)]tetraacetic acid; MAP, microtubule associated protein; MES, 2-[*N*-morpholino]-ethane sulfonic acid; MTP, microtubule protein composed of tubulin and MAPs, primarily MAP2 and tau; PC-tubulin, MAP-free phosphocellulose purified tubulin; Pipes, piperazine-*N*,*N*′-bis(2-ethanesulfonic acid); avlb, anhydrovinblastine; vcr, vincristine; vfl, vinflunine; vlb, vinblastine; vrb, vinorelbine.

10.1021/bi001038r CCC: $19.00
Published on Web 09/02/2000

A

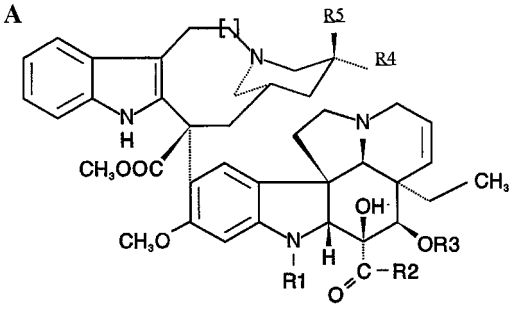

	R1	R2	R3	R4	R5	[ ]
Vincristine	CHO	OCH_3	$COCH_3$	CH_2CH_3	OH	----
Vinblastine	CH_3	OCH_3	$COCH_3$	CH_2CH_3	OH	----

B

Structure	Code	ΔΔG
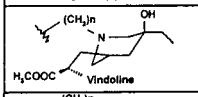	n = 2 VINBLASTINE F 80302	0.00
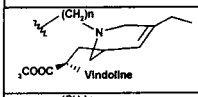	n = 2 AVLB F 81097	0.07 ±0.18
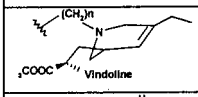	n = 1 VINORELBINE F 80520	0.58 ±0.28
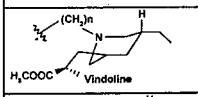	n = 1 F 91671	0.65 ±0.16
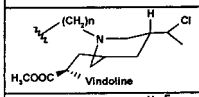	n = 1 F 13840	0.99 ±0.08
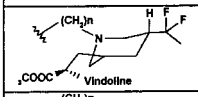	n = 1 VINFLUNINE	1.20 ±0.29
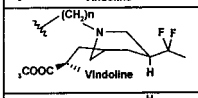	n = 2 F 91642	1.33 ±0.07
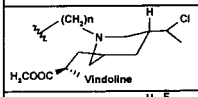	n = 2 F 13667	1.34 ±0.10
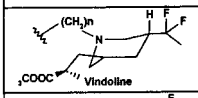	n = 2 F 12844	1.55 ±0.04
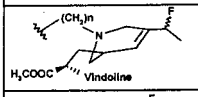	n = 1 F 91641	1.95 ±0.21
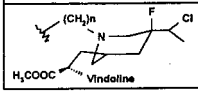	n = 2 F 91183	>> no spirals

FIGURE 1: Chemical structures of test compounds. (A) Vincristine is compared to vinblastine, and (B) in column form, the vinblastine modifications on the various cathranthine moieties are indicated in column 1, with the compound designation in column 2, and the decrease in spiraling potential in free energy units relative to vinblastine ($\Delta\Delta G$, averaged over the GTP and GDP conditions) is listed in column 3. Relative to vinblastine, the CHO substitution at R1 on vincristine enhances spiraling potential, $\Delta\Delta G = -0.91 \pm 0.17$ kcal/mol.

C-20′ position with loss of the 3′,4′ double bond. Only a few studies have investigated how specific chemical modifications affect drug activity in cell culture. Owellen and co-workers investigated the effect of chemical modifications on 11 vinblastine congeners on partition coefficients and drug activity (*10*). Apparent binding affinities were determined from competition experiments with ^{3}H-vinblastine. In animal studies, partition coefficients and apparent binding affinities correlated with drug LD_{50} and anti-P388 activity. The activities of 10 C-20′ congeners of vinblastine were evaluated by Borman and co-workers (*11*, *12*). Differences in potency in terms of cell growth inhibition and mitotic arrest correlated with inhibition in vitro of microtubule protein (MTP) assembly. Thus, it appears that binding affinities, microtubule inhibition, and lipophilicity may be important contributors to vinca alkaloid activity.

We present here a quantitative structure−activity study of vinblastine, vincristine, vinorelbine, anhydrovinblastine, vinflunine, and a series of vinflunine derivatives (Figure 1). We examined in vitro drug binding, microtubule inhibition, and lipophilicity as determined by octanol−water partition coefficients. We used sedimentation velocity data fit with the Wyman linkage model to obtain precise estimates of overall drug binding and spiraling potential. We demonstrate that, for these compounds, L1210 cell culture IC_{50} values are most closely correlated with vinca alkaloid-induced tubulin spiral formation. Surprisingly, for these compounds, microtubule inhibition is not a predictor of cytotoxicity.[2]

MATERIALS AND METHODS

Reagents. $MgSO_4$, EGTA, GTP (Type II-S), glycerol, MES, octanol, and vincristine sulfate were purchased from Sigma Chemical Company. Sephadex G-50 was from Pharmacia. Deionized (Nanopure) water was used in all experiments.

Synthesis of Compounds. The compounds used in these studies are listed in Table 1. These compounds, with the exception of vincristine, have modifications of the cleavamine moiety of the basic vinblastine structure (*13*, *14*). There are four features that are explored: the conversion of a nine-membered ring ($n = 2$) to an eight-membered ring ($n = 1$); the replacement of an -OH at R5 with a hydrogen, a fluorine atom (-F) or a double bond in the piperidine ring; the substitution of a mono-F, mono-Cl, or di-F at R4; or a combination of these modifications.

Tubulin Purification. Purified tubulin (PC-tubulin) free of MAPs was obtained by warm/cold polymerization/depolymerization with the addition of a final phosphocellulose chromatography step to separate tubulin from MAPs (*15*, *16*). Protein concentrations were determined spectrophotometrically ($\epsilon_{278} = 1.2$ L/g cm) (*17*).

Sedimentation Velocity Experiments. Vinblastine sulfate, vincristine sulfate, 3′,4′-anhydrovinblastine di(hydrochloride), and the ditartrate salts of vinorelbine, vinflunine, and vinflunine derivatives (Table 1) were studied in the presence of GDP or GTP by sedimentation velocity. Tubulin samples (2 μM) were equilibrated in 10 mM MES, pH 6.9, 2 mM EGTA, 1 mM $MgSO_4$, 50 μM GXP using spun columns. (This buffer differs from our previous studies in 10 mM Pipes because a few of these compounds, especially F 12844 and

[2] We will use the term "cytotoxicity" to indicate the magnitude of the antiproliferative effects on L1210 cells induced by test compounds. We prefer this usage over "potency" because it does not tend to suggest efficacy. In fact, it is possible that less cytotoxic vinca alkaloids may be more valuable in clinical use due to reduced toxicity to normal cells and an increased therapeutic index.

Table 1: Partition Coefficients, Microtubule Inhibition, and Cytotoxicity for All Test Compounds

	log P calculated	log P measured	microtubule inhibition purified tubulin IC_{50} μM	microtubule inhibition MTP IC_{50} μM	cytotoxicity L1210 cells IC_{50} nM
vincristine sulfate	4.1	1.16 (± 0.02)	0.45 (± 0.06)	1.5	16
vinblastine sulfate	5.4	1.89 (± 0.01)	0.37 (± 0.02)	2.6	16
F81097: 3′,4′-anhydrovinblastine di(hydrochloride)	5.8	1.34 (± 0.05)	0.32 (± 0.02)	0.7	170
vinorelbine ditartrate	3.1	1.32 (± 0.01)	0.44 (± 0.04)	1.5	28
F91671: (4′R)3′,4′′dihydrovinorelbine ditartrate	3.8	0.57 (± 0.01)	0.31 (± 0.04)	1.0	27
F13840: 20′-chloro-3′,4′-dihydrovinorelbine ditartrate	3.9	1.20 (± 0.01)	0.30 (± 0.04)	0.9	23
vinflunine ditartrate	4.3	1.27 (± 0.01)	0.49 (± 0.05)	3.5	97
F91642: (4′S)20′,20′-difluoro-′4′-deoxyvinblastine ditartrate	6.8	1.14 (± 0.01)	0.39 (± 0.04)	1.7	470
F13667: 20′-chloro-4′-deoxyvinblastine ditartrate	6.5	1.81 (± 0.01)	0.38 (± 0.02)	2.0	360
F12844: (4′R)20′,20′-difluoro-′4′-deoxyvinblastine ditartrate	7.0	2.02 (± 0.02)	0.35 (± 0.04)	2.5	390
F91641: 20′-fluorovinorelbine ditartrate	2.7	1.21 (± 0.01)	0.66 (± 0.01)	3.4	490
F91183: 20′-chloro-4′-deoxy-4′-fluorovinblastine ditartrate	7.0	1.16 (± 0.01)	0.89 (± 0.03)	1.5	>1000

F 91183, exhibited limited solubility in Pipes vs MES.) The free compound concentration (0.5−70 μM) was obtained from the known compound concentration in the equilibration buffer. The following extinction coefficients were used to determine test compound concentrations: vinblastine $\epsilon_{320,\,water} = 4647\ M^{-1}\ cm^{-1}$; vincristine $\epsilon_{296,\,ETOH} = 15136\ M^{-1}\ cm^{-1}$; vinflunine, F 13840, F 91671, $\epsilon_{268,\,water} = 18650\ M^{-1}\ cm^{-1}$; vinorelbine, F 91641, $\epsilon_{268,\,water} = 17150\ M^{-1}\ cm^{-1}$; F 81097 $\epsilon_{268,\,water} = 18200\ M^{-1}\ cm^{-1}$; F 12844, F 13667, F 91642, F 91183, $\epsilon_{268,\,water} = 19960\ M^{-1}\ cm^{-1}$. After equilibration, the protein was brought to the desired final concentration by dilution with the equilibration buffer. Sedimentation studies were done in a Beckman Optima XLA analytical ultracentrifuge equipped with absorbance optics and an An60 Ti rotor. Samples were spun at 25 °C at appropriate speeds. Velocity data were collected at 278 nm and at a spacing of 0.002 cm with 1 average in a continuous scan mode. Data were analyzed using software (DCDT) provided by Dr. Walter Stafford (Boston Biomedical Research Institute) to generate a distribution of sedimentation coefficients, $g(s)$.

Curve Fitting of Sedimentation Velocity Data. The distributions of sedimentation coefficients, $g(s)$, were converted to weight average $\bar{s}_{20,w}$ values as described (*16*, *18*, *19*). Sedimentation data were fit using the isodesmic ligand-mediated model. In this model, K_1 is the affinity of drug for tubulin heterodimers, and K_2 is the affinity of liganded-heterodimers for spiral polymers. Binding constants and error estimates were obtained by fitting with the nonlinear least squares program Fitall (MTR software, Toronto, Canada), modified to include the appropriate fitting functions. Simulations of weight average S and spiral molecular weight were performed by using the fitting routine to generate data at a fixed protein concentration and over a range of drug concentrations for specific sets of K_1K_2 parameters (see Tables 2 and 3).

Microtubule Inhibition. PC-tubulin (1.8 mg/mL) was polymerized in 100 mM MES, pH 6.9, 10 mM $MgSO_4$, 2 mM EGTA, 1 mM GTP, and 2 M glycerol. Experiments were carried out in the presence and absence of test compounds over concentration ranges of 0.1 to 1 μM. Microtubule formation was monitored using a Gilford Response II UV−Vis or a Varian Cary 3E scanning spectrophotometer equipped with a cooling Peltier cell holder. Prior to polymerization, samples were degassed on ice for 30 min, and baseline data were collected at 4 °C and 350 nm. The temperature was increased to 37 °C, and solutions were monitored at 350 nm for 45 min. Solutions were cooled to 0 °C, and a second baseline was recorded. The change in optical density was plotted vs compound concentration after subtracting the second baseline from the plateau optical density at 45 min. This ΔOD corresponds to the temperature-sensitive reversible polymerization and corrects for irreversible aggregation. The percent inhibition was calculated relative to the control sample. The IC_{50} concentration (drug concentration causing 50% inhibition of microtubule assembly) was determined from the mean of three independent experiments.

In addition, experiments were performed with MAP containing whole microtubule protein samples. MAPs, primarily MAP2 and tau in these solutions, stabilize microtubules and are likely to resist the actions of depolymerizing drugs such as the vinca alkaloids. Any differential effects of vincas may reflect differential interactions with this class of MAPs (*20*). Experiments were performed as described previously (*21*).

Linear Regression Fit of the Data. Log K_1K_2, log IC_{50}, and log P data were fit by linear regression using Origin 5.0 (Microcal Software Inc., Northampton, MA). Using this software, statistical significance is determined by t-test. The p values reported are for t-test of the slope = 0. A p value ≤ 0.05 is considered to be statistically significant.

Partition Coefficients. Partition coefficients for the compounds in octanol and water were measured as described by Owellen and co-workers (*10*). The solutions were buffered at pH 6.9 in 10 mM MES, pH 6.9, 2 mM EGTA, 1 mM $MgSO_4$, and 0.05 mM GTP. The compound concentrations in the octanol and water phases were determined using the extinction coefficients as listed above. Measurements for each compound were carried out in triplicate, and the means and standard deviations were determined. Partition coefficients, corresponding to the Molecular Lipophilicity Potential (CLIP 1.0 software, Institute of Medicinal Chemistry, University of Lausanne, Switzerland), were also calculated. The origin of the observed difference between measured and calculated partition coefficients reflects, in part, the fact that calculated log P corresponds to an extrapolation of the partition coefficient of the test compound considered as the free base (Table 1). Similar deviations have been observed for other compounds and software packages, and it is possible these compounds lie outside the optimal prediction space for CLIP 1.0 (*22*, *23*).

Table 2: Equilibrium Constants for the Interaction of Vinca Alkaloids with Tubulin and GTP[a]

drug	K_1 (M^{-1})	K_2 (M^{-1})	K_1K_2 (M^{-2})	SD[b]
vincristine	$1.9 \times 10^5 \pm 0.5$	$2.7 \times 10^7 \pm 0.4$	4.9×10^{12}	2.2
vinblastine	$1.1 \times 10^5 \pm 0.2$	$8.2 \times 10^6 \pm 0.8$	8.6×10^{11}	0.9
F 81097	$1.8 \times 10^5 \pm 0.4$	$5.3 \times 10^6 \pm 0.6$	9.5×10^{11}	1.2
vinorelbine	$9.5 \times 10^4 \pm 1.7$	$2.4 \times 10^6 \pm 0.3$	2.3×10^{11}	0.6
F 91671	$9.5 \times 10^4 \pm 1.7$	$2.6 \times 10^6 \pm 0.3$	2.4×10^{11}	0.6
F 13840	$1.3 \times 10^5 \pm 0.0$	$1.3 \times 10^6 \pm 0.0$	1.8×10^{11}	0.4
vinflunine	$4.3 \times 10^5 \pm 0.9$	$3.9 \times 10^5 \pm 0.2$	1.6×10^{11}	0.2
F 91642	$8.2 \times 10^4 \pm 2.3$	$1.2 \times 10^6 \pm 0.2$	9.8×10^{10}	0.3
F 12844	$5.1 \times 10^4 \pm 2.1$	$1.2 \times 10^6 \pm 0.4$	6.0×10^{10}	0.7
F 13667	$1.1 \times 10^5 \pm 0.2$	$9.6 \times 10^5 \pm 1.0$	1.0×10^{11}	0.4
F 91641	$1.4 \times 10^5 \pm 0.3$	$2.9 \times 10^5 \pm 0.3$	4.1×10^{10}	0.2
F 91183				

[a] 10 mM MES, pH 6.9, 2 mM EGTA, 1 mM $MgSO_4$, 0.05 mM GTP (25 °C). Data were fit with the ligand-mediated model. [b] SD is the standard deviation of the fit.

Table 3: Equilibrium Constants for the Interaction of Vinca Alkaloids with Tubulin and GDP[a]

drug	K_1 (M^{-1})	K_2 (M^{-1})	K_1K_2 (M^{-2})	SD[b]
vincristine	$2.0 \times 10^5 \pm 0.03$	$8.1 \times 10^7 \pm 0.7$	1.6×10^{13}	1.8
vinblastine	$1.5 \times 10^5 \pm 0.04$	$2.7 \times 10^7 \pm 0.04$	4.2×10^{12}	1.5
F 81097	$1.2 \times 10^5 \pm 0.2$	$2.5 \times 10^7 \pm 0.3$	3.0×10^{12}	1.7
vinorelbine	$2.5 \times 10^5 \pm 0.6$	$8.7 \times 10^6 \pm 0.8$	2.2×10^{12}	1.3
F 91671	$1.7 \times 10^5 \pm 0.4$	$1.0 \times 10^7 \pm 0.1$	1.7×10^{12}	1.3
F 13840	$1.7 \times 10^5 \pm 0.3$	$4.3 \times 10^6 \pm 0.4$	7.2×10^{11}	0.8
vinflunine	$2.0 \times 10^5 \pm 0.4$	$2.0 \times 10^6 \pm 0.2$	3.9×10^{11}	0.7
F 91642	$1.7 \times 10^5 \pm 0.4$	$2.4 \times 10^6 \pm 0.3$	4.1×10^{11}	0.8
F 12844	$8.9 \times 10^4 \pm 2.0$	$3.6 \times 10^6 \pm 0.5$	3.2×10^{11}	0.8
F 13667	$1.2 \times 10^5 \pm 0.2$	$3.3 \times 10^6 \pm 0.4$	3.9×10^{11}	0.8
F 91641	$9.9 \times 10^4 \pm 1.9$	$1.3 \times 10^6 \pm 0.1$	1.2×10^{11}	0.5
F 91183				

[a] 10 mM MES, pH 6.9, 2 mM EGTA, 1 mM $MgSO_4$, 0.05 mM GDP (25 °C). Data were fit with the ligand-mediated model. [b] SD is the standard deviation of the fit.

Cell Culture Studies. The cytotoxicity data for each compound were determined using L1210 cells and 48 h test compound exposures. The effects on cell proliferation were monitored using a standard growth inhibition assay, based on cell counting, as described by Kruczynski and co-workers (*21*).

RESULTS

Binding to Tubulin Heterodimers: K_1. Tables 2 and 3 show the equilibrium constants, determined from data collected by sedimentation velocity, for the test compounds. Equilibrium constants were obtained from fits with the ligand-mediated model. As observed in previous studies (*6*), there is no significant difference in K_1, the affinity of test compounds for tubulin heterodimers. The mean affinity of these compounds for tubulin heterodimers is $1.5 \times 10^5 \pm 0.8$ M^{-1}. One test compound, F 91183, does not induce tubulin spirals; therefore, we cannot determine equilibrium constants for this compound using sedimentation velocity. Because of the very low affinity of this compound for tubulin, we were also unable to determine the affinity of F 91183 for tubulin heterodimers using the intrinsic tubulin fluorescence (*24*). We cannot exclude the possibility that changes in fluorescence are induced by spiral formation rather than by vinca binding (*6*). Consistent with this hypothesis, we have recently demonstrated that under the fluorescence conditions previously thought to suppress vinca-induced spirals (absence of Mg^{2+} at 2.85 μM tubulin concentration; refs *25* and *26*) measurable vinblastine-induced tubulin self-association does occur, albeit weakly (*6*).

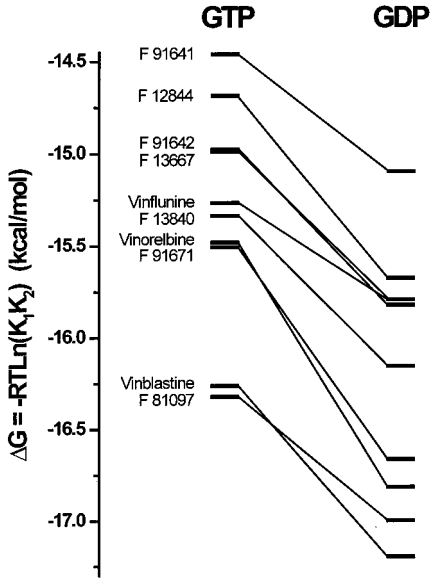

FIGURE 2: Free energy of overall spiraling potential ($\Delta G = -RT\ln K_1K_2$) is plotted for GTP and GDP conditions. The GDP enhancement of drug-induced spiraling ($\Delta\Delta G = 0.86 \pm 0.23$ kcal/mol) is evident by the shift to more negative values. K_1K_2 values, determined from ligand-mediated fits, are listed in Tables 2 and 3. For clarity of presentation, vincristine is not included.

Comparison of Vinca-Induced Tubulin Spiral Size: K_1K_2. The apparent tubulin spiraling potentials, K_1K_2, induced by all the test compounds studied are given in Tables 2 and 3. Note that because K_1 is relatively constant for all test compounds, the spiraling potential and the average spiral size, reflected by K_1K_2, is largely determined by K_2. Vincristine induces the largest tubulin spirals, and F 91641 induces the smallest tubulin spirals. For example, K_1K_2 values for these compounds are 4.9×10^{12} and 4.1×10^{10} M^{-2} for GTP conditions and 1.6×10^{13} and 1.2×10^{11} M^{-2} for GDP conditions. The free energy for spiral formation, ΔG, is calculated from the overall spiraling potential, K_1K_2. GDP enhances vinca-induced tubulin spiraling with a mean $\Delta\Delta G = 0.86 \pm 0.23$ kcal/mol (Figure 2). This change in free energy, $\Delta\Delta G$, is determined by subtracting ΔG in the presence of GDP from ΔG in the presence of GTP ($\Delta G_{gtp} - \Delta G_{gdp}$). This result is similar to our previous findings (*7*, *8*, *18*) and indicates that propagation of vinca-induced tubulin spirals into the microtubule GDP core should be favored under all conditions studied. Note that the tubulin spiraling potential, K_1K_2, for the combined nucleotide and vinca alkaloid data, ranges from 4.1×10^{10} ($\pm$ 1.0) to 1.6×10^{13} ($\pm$ 0.1) M^{-2}, representing a 390-fold difference. Thus, the $\Delta\Delta G$ due to these allosteric effectors is equal to about 3.53 kcal/mol. As noted above, these differences in spiraling potential are largely due to changes in the ability of tubulin to self-associate, K_2, rather than in the affinity of vinca for tubulin heterodimers, K_1. There is only an 8.4-fold difference in K_1 values ranging from 0.5×10^5 ($\pm$ 0.2) to 4.3×10^5 ($\pm$ 0.9) M^{-1}, and in fact, most K_1 estimates, 1.5 ($\pm$ 0.8) $\times$ 10^5 M^{-1}, agree to within a factor of 2. This corresponds to a ΔG_{K1} value of -7.06 ± 0.30 kcal/mol and, combined with the 8.4-fold range, gives a range of $\Delta\Delta G_{K1}$ values of approximately 0.6 to 1.3 kcal/mol. This leaves 2.93−2.27

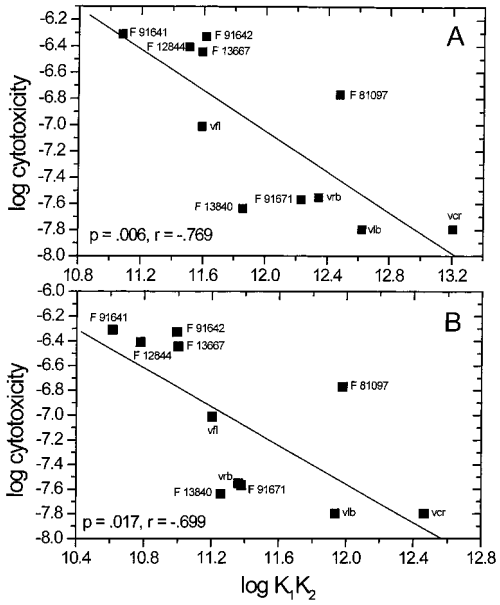

FIGURE 3: Plot of log K_1K_2 vs log cytotoxicity for sedimentation velocity data collected in the presence of (A) GDP or (B) GTP. Data were fit by linear regression using Origin 5.0 to obtain p and r, the correlation coefficient.

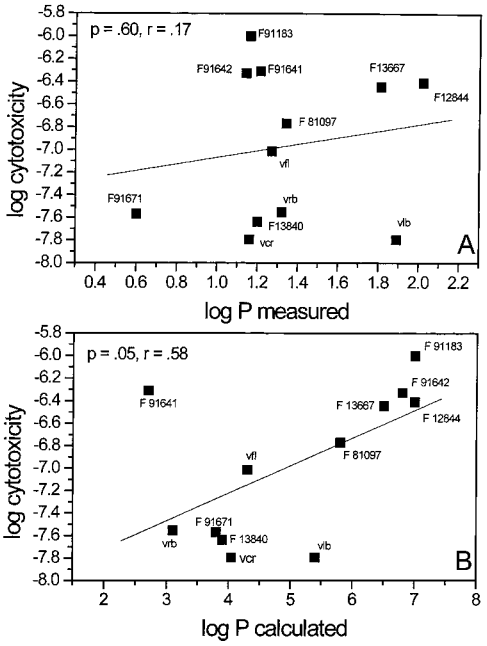

FIGURE 4: Plot of (A) measured log P and (B) calculated log P vs log cytotoxicity. Data were fit by linear regression using Origin 5.0.

kcal/mol due to differences in K_2, $\Delta\Delta G_{K2}$, the self-association step. We therefore conclude that these allosteric effectors, nucleotide and vinca alkaloid, act by altering primarily the potential for tubulin heterodimers to self-associate without significantly affecting the strength of vinca binding. This result implies that the binding site for vinca alkaloids is intimately connected to the self-association process, consistent with our hypothesis that the site is structurally located between dimers (*6*). To emphasize the linkage of spiraling potential to average spiral size, we can simulate the situation for the strongest spiraling conditions, vincristine and GDP, versus the weakest spiraling conditions, F 91641 and GTP. At 0.2 mg/mL tubulin and 50 μM test compound, the weight average sedimentation coefficients are 44.5 and 8.0 *S*, respectively and correspond to a weight average spiral size of 23.2 vs 1.7 tubulin heterodimers.

Spiral Size and Cytotoxicity. To explore the significance of drug-induced tubulin spiraling and inhibition of cell proliferation, we compared tubulin spiraling potential and the effect of test compounds on leukemic L1210 cells. The cytotoxicity IC_{50} data range from 16 nM for the most cytotoxic (vincristine) to 490 nM for the least cytotoxic (F 91641) (Table 1). There is a statistically significant linear correlation ($p = 0.006$ to 0.017) between spiraling potential, as indicated by log K_1K_2, and log cytotoxicity in L1210 cells (Figure 3). Larger K_1K_2 values and thus larger spirals correlate with lower IC_{50} values. This result is verified even for the compound that does not induce spirals, F 91183, since its cytotoxicity is negligible being reported as >1000 nM. Cytotoxicity has been correlated with the cellular lifetime or intracellular retention of the agent (*27*). We have previously shown that large spiraling potential correlates with slow relaxation times in stopped flow experiments (*7*, *18*). This observation is consistent with large spiral polymers dissociating by a cascade of steps that slows down the release of both free tubulin and drug. Thus, we hypothesize that the intracellular lifetimes of vincas are determined in part by the size of the tubulin spirals induced. Test compounds that induce larger spirals tend to be more cytotoxic because drug molecules are trapped in tubulin oligomers and released only as the spirals depolymerize. Larger spiral size thus results in longer intracellular exposure to the test compound. This phenomenon accounts for the ability of cells to concentrate vinca alkaloids (*4*) and essentially buffers the cellular concentration of a cytotoxic agent. Note that the L1210 cell line used in our studies does not express p-glycoprotein that would presumably counteract the intracellular concentrating effect of drug-induced tubulin spirals.

Partition Coefficients and Cytotoxicity. The work of Owellen and co-workers indicated that lipophilicity and cellular uptake may be important contributors to passive cellular diffusion and cytotoxicity (*10*). We therefore measured the partition coefficients for all the compounds studied. We also calculated the partition coefficients corresponding to the Molecular Lipophilicity Potential (CLIP 1.0 software, Institute of Medicinal Chemistry, University of Lausanne, Switzerland). In agreement with previous studies, cytotoxicity data are correlated with calculated partition coefficients (Table 1, Figure 4, panel B, $p = 0.05$), but there is no statistically significant correlation for measured values (Figure 4, panel A, $p = 0.60$), even by introducing corrections reflecting the distribution of free base alone, as described by Owellen and co-workers (data not shown; ref *10*). It is of interest that the correlation of the calculated log P data suggests cytotoxicity is improved by decreased lipophilicity and increased aqueous solubility.

Microtubule Inhibition and Cytotoxicity. There is no significant correlation between microtubule inhibition using purified tubulin and cytotoxicity (Figure 5, $p = 0.09$). These data include F 91183, which from cytotoxicity measurements has an IC_{50} that is >1000 nM; therefore, a value of 1000 nM is included in the analysis in Figure 5. There is also no significant correlation between inhibition of microtubule protein assembly and cytotoxicity (Table 1; $p = 0.44$; $r = 0.26$). Assembly with MTP presumably corresponds to a

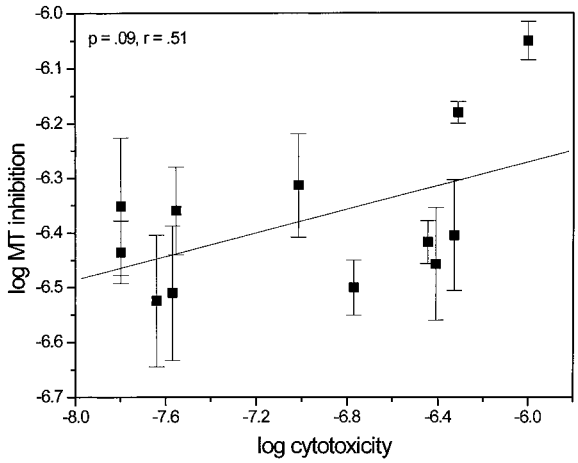

FIGURE 5: Plot of log microtubule inhibition (purified tubulin) vs log cytotoxicity to obtain *p* and *r*, the correlation coefficient.

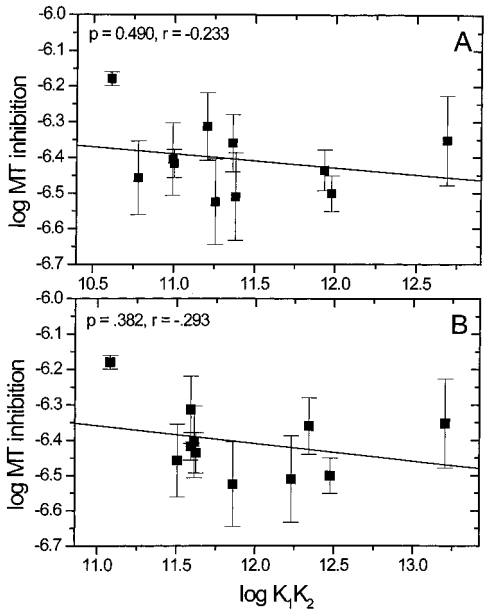

FIGURE 6: Plot of log microtubule inhibition (purified tubulin) vs log K_1K_2 for sedimentation velocity data collected in the presence of (A) GTP or (B) GDP. Data were fit by linear regression using Origin 5.0 to obtain *p* and *r*, the correlation coefficient. Because F 91183 does not induce tubulin spiral formation, it is not included in this plot.

more cellular mixture of proteins and thus reflects a more cellular response to drugs (see Discussion). Although microtubule inhibition studies have been commonly used to evaluate vinca alkaloid potency in cell culture, our studies suggest that for these compounds, it is not a predictor of cytotoxicity in L1210 cells, as reported earlier for PtK2 cells (*28*).

Microtubule Inhibition and Spiral Size. There is no statistically significant correlation between microtubule inhibition using purified tubulin and spiral size (K_1K_2) for data collected in the presence of GTP ($p = 0.49$) or GDP ($p = 0.38$) (Table 1, Figure 6). Microtubule inhibition IC_{50} values, range from 0.30 ± 0.04 μM for F 13840 (the most inhibitory) to 0.89 ± 0.03 μM for F 91183 (the least inhibitory). There is also no significant correlation between MTP inhibition data and the spiral size (Table 1), although the trends are slightly better (GDP data; $p = 0.11$, $r = -0.51$; GTP data, $p = 0.15$, $r = -0.47$). Because F 91183 does not induce measurable tubulin spirals, the data from this test compound are not included in the analysis in Figure 6.

All but two IC_{50} values in Table 1 and Figure 6 fall within a fairly narrow range, between 0.30 and 0.49 μM. It should be noted that under our polymerization conditions for purified tubulin in 2 M glycerol and the MTP samples, the microtubules do not exhibit significant dynamic instability. Thus, these stabilized microtubules are not significantly affected by changes in vinca-induced tubulin spiral size. It is possible that dynamic mitotic microtubules are more sensitive to disruption by vinca alkaloids and that the inhibition of dynamic microtubules at equitoxic doses would correlate with cytotoxicity.

DISCUSSION

Drug-Induced Tubulin Spiral Size and Cytotoxicity. The results presented here agree well with previous studies demonstrating that vinca alkaloids bind with similar affinity to tubulin heterodimers, $K_1 = 1.5 \times 10^5 \pm 0.8$ (*8*). Therefore, the reason for their differential activity and toxicity is not due to differential affinity for tubulin heterodimers. Drug binding, however, is linked to tubulin spiral formation (*5*), and this provides the major component of the 390-fold range of values observed for the strongest to the weakest spiraling potential. Synthesis of vinca alkaloids requires the coupling of two precursors, a vindoline portion and a catharanthine portion that rearranges into a cleavamine nucleus during synthesis. To understand how each moiety may contribute to drug activity, their potentials for inducing tubulin spirals and inhibiting microtubule formation in vitro were investigated separately (*26*). The catharanthine moiety was demonstrated to retain the ability to induce spiral formation ($K_2 = 1.0 \times 10^5$ M^{-1}) but it had weak affinity for tubulin heterodimers ($K_1 = 2.8 \times 10^3$ M^{-1}). The overall spiraling potential of catharanthine was 3.8 kcal/mol weaker than vinflunine (as measured in this study). (It should be mentioned that the structure of catharanthine itself is markedly different from that of cleavamine included into the dimeric vinca alkaloids. Thus activities reported for catharanthine might not be directly related to those in the dimers.) The vindoline moiety (the "lower" half of the dimer of rings) must be present to achieve 100% of the drug efficacy and was assigned the role of anchoring the drug to the binding site. All the test compounds in our studies except vincristine differed by chemical modifications of the catharanthine moiety. Thus, we have demonstrated that these modifications do not significantly affect the affinity of drug for tubulin; however, they do have an important impact on drug-induced tubulin spiraling.

Relative to vinblastine, the smallest change in spiraling potential occurs for anhydrovinblastine, F 81097, which corresponds to the dehydration of the alcohol function of vinblastine: F 81097 has nearly identical spiraling potential to vinblastine, $\Delta\Delta G = 0.071 \pm 0.181$ kcal/mol, after OH removal and double bond formation in the ring. (The data in Figure 1, panel B, and Table 1 are listed in order from strongest to weakest spiraling potential to facilitate relating structural changes to energetic consequences.) Surprisingly, F 81097 is the single outlier in the cytotoxicity data, being much less cytotoxic than vinblastine, 170 vs 16 nM. Alternatively, F 91671 retains strong spiraling potential

relative to vinblastine ($\Delta\Delta G = 0.647 \pm 0.156$ kcal/mol) after two modifications (an OH to H substitution at R5 and a reduction in ring size, $n = 2$ to $n = 1$), and it also is highly cytotoxic, 27 nM. The conversion of F 91671 to vinflunine adds two fluorines to R4, which doubles the impact on spiraling potential relative to vinblastine ($\Delta\Delta G = 1.202 \pm 0.291$ kcal/mol) while retaining modest cytotoxicity, 97 nM. F 12844 is essentially vinflunine with the nine-membered ring ($n = 2$) of vinblastine. This actually weakens spiraling potential relative to vinblastine ($\Delta\Delta G = 1.551 \pm 0.037$ kcal/mol) and significantly reduces cytotoxicity, 390 nM. Thus, an $n = 2$ to $n = 1$ modification partially compensates for the influence of -OH removal at R5 and di-F addition at R4. For vinflunine relative to F 12844, $\Delta\Delta G = -0.349 \pm 0.328$ kcal/mol. An $n = 2$ to $n = 1$ conversion occurs in two other instances in these data. In one case, it favors spiraling, and in another case, it disfavors spiraling. F 13840 ($n = 1$) and F 13667 ($n = 2$) differ only by the size of this ring, and F 13840 has a larger spiraling potential relative to F 13667 ($\Delta\Delta G = -0.356 \pm 0.011$ kcal/mol). Alternatively, vinorelbine ($n = 1$) has a weaker spiraling potential relative to avlb or F 81097 ($n = 2$) ($\Delta\Delta G = 0.511 \pm 0.464$ kcal/mol). As discussed below, this may reflect an unfavorable coupling to the double bond (*29*). Comparing F 91642 with F 12844 demonstrates that inversion of the C4′ configuration is not a critical feature associated with spiraling potential ($\Delta\Delta G = 1.331 \pm 0.065$ kcal/mol relative to vinblastine and $\Delta\Delta G = -0.219 \pm 0.110$ kcal/mol relative to F 12844). F 91641 is essentially vinorelbine substituted with a single-F at R4; this modification dramatically reduces the spiraling potential relative to vinblastine ($\Delta\Delta G = 1.954 \pm 0.214$ kcal/mol vs only $\Delta\Delta G = 0.582 \pm 0.281$ kcal/mol for vinorelbine) and reduces the cytotoxicity to 490 nM. Placing even a single electronegative atom such as a fluorine atom in a more rigid ring orientation causes a considerable reduction in spiral stability. A double halogen substitution at R5 and R4 in F 91183 completely abolishes tubulin binding, spiral formation, and cytotoxicity (>1000 nM). Thus, this portion of the drug, R4 and R5, may be interacting with a hydrogen bond acceptor or an electrophilic region on the protein that electrostatically interacts unfavorably with the -F and -Cl substitutions of this family of compounds. Introduction of rigidity or multiple sites of substitution is significantly less favorable for spiraling.

A series of previous papers by Borman and co-workers investigated 10 different C-20′ modified vinblastine derivatives (*11*, *12*). The modifications involved removal of the R5−OH in combination with removal of the R4-ethyl, replacement of the ethyl with methyl or propyl, and epimeric versions of these substitutions at the R4−R5 position. These compounds are most similar to avlb (F 81097), vinorelbine, and F 91671 in our study because no dramatic electrophilic additions occurred. Borman and Kuehne's compounds (*12*) could be split into two groups, those with small effects and those with dramatic effects on microtubule and cell growth inhibition. For example, replacement of ethyl with methyl, removal of the hydroxyl and the epimeric forms of these chemical changes have no significant effects. This parallels our conclusions and further argues that the R5-OH has no significant favorable interactions in the binding pocket. Alternatively, removal of the R4-ethyl, both the R5-OH and the R4-ethyl, or the substitution of a propyl increases the MTP IC_{50} values by an order of magnitude and weakens cytotoxicity by 1−2 orders of magnitude. Thus, creation of an unfilled pocket or expansion of the ethyl moiety to propyl at either R4 or R5 disrupts tubulin binding. (Because of the close linkage between binding and spiral formation, we would anticipate a significant effect on spiral formation for these compounds.) This creates two clusters of data in a log MTP IC_{50} vs log cytotoxicity plot of the Borman and Kuehne results. A linear fit gives a significant correlation with p values <0.001, consistent with their conclusions that MTP inhibition correlates with cytotoxicity. However, within each cluster, weak or strong inhibitors, there is no obvious trend or significant correlation. In fact, our data (Figure 5) are very similar to the strong inhibitors in the Borman data set with both sets exhibiting a relatively flat, zero slope, correlation plot with microtubule inhibition data agreeing within a factor of 2 and cytotoxicity varying by orders of magnitude. This allows us to suggest that previous correlation studies must be viewed with caution depending upon the nature of the set of compounds investigated. Clearly, sedimentation studies on these derivatives (*12*) are required before we can definitively assert that spiraling potential is the more accurate measure of cytotoxicity for other vinca alkaloid congeners.

A more quantitative and molecular interpretation of these data requires two additional components. First, we do not know the high-resolution molecular features of the vinca alkaloid binding site in a spiral. The taxol-tubulin binding site is currently being refined to high resolution (E. Nogales, personal communication), but vinca binding and spiral formation disrupts the two-dimensional tubulin sheets or crystals used to solve the electron diffraction structure. Thus, high resolution structural data on the vinca binding site must await new experimental developments. Second, DiCera has described methods of deciphering the linkage between various modifications of a drug or substrate (*29*). The method requires a series of thermodynamic cycles where modifications are made singly and then in combination, thus allowing a determination of additive or cooperative linkages that influence the binding or association process. For example, the $n = 2$ to $n = 1$ transition data suggests a complex linkage to other changes in the structure, possibly mediated by changes induced in the drug binding pocket. Alternatively, the enhancement by GDP ($\Delta\Delta G = 0.86 \pm 0.23$ kcal/mol) observed in all vinca alkaloids derivatives tested thus far, within error, is an additive linkage to vinca-induced spiraling and suggests the absence of any significant cooperative effects. Nonetheless, by a similar energetic analysis, we are able to suggest the influence specific chemical modifications at the C-20′ position of vinblastine have on spiraling potential. A more rigorous analysis of these data requires a far more extensive study of vinca derivatives by similar methods. Unfortunately, many of the required derivatives have proven to be difficult to synthesize (*14*). In addition, only future structural information on the vinca binding site will allow us to verify and interpret the role of important protein side chain components in this drug-induced association process.

Although clinical data is limited to four of the compounds discussed here (vincristine, vinblastine, vinorelbine, and vinflunine), it is interesting to speculate on how the data presented here may be related to clinical findings. It should be noted, however, that additional pharmacokinetic and

pharmacodynamic factors, such as drug transporters and alternate drug targets, are likely to contribute to clinical efficacy. Of the drugs currently in clinical use, vincristine, given at the lowest doses, and vinflunine, given at the highest doses, differ by 30−40-fold in their potential to induce tubulin spirals, K_1K_2, (Tables 2 and 3). For the 12 test compounds examined in these studies, we have demonstrated that tubulin spiral size is the best predictor of L1210 cell cytotoxicity. Compounds that induce the largest tubulin spirals tend to have the lowest L1210 IC_{50} values (Figure 3). How might drug-induced tubulin spiral size be directly linked to cytotoxicity? As tubulin spirals form, vinca alkaloids bind at the α- and β-interface between two dimers and are trapped within the spirals (*6*). We have shown previously, using light scattering, that relaxation times of vincristine-induced tubulin spiral dissociation are more than 10-fold longer than those of vinblastine, vinorelbine, or vinflunine (*7*, *8*, *30*). Larger spirals sequester more vinca alkaloid molecules. This accounts for the ability of cells to concentrate vinca alkaloids (*4*). For drugs to be released from cells, spirals must depolymerize, releasing drug and tubulin heterodimers. Free drug can then passively diffuse or be actively transported from the cell. Since the time needed for drug release is determined by the spiral size, the intracellular lifetime of vinca alkaloids will be longer for those that induce larger tubulin spirals. Thus, spiral formation essentially buffers the cellular drug concentration leading to increased cytotoxicity. In addition, the cellular location of spiral formation may play a role in this mechanism. If at clinical doses spirals preferentially form at microtubule ends then the spiral size and stability magnifies the effect on dynamics suppression and becomes a direct measure of differential cytotoxicity. Future in vitro and cellular studies on the location of fluorescently labeled vincas, if the modification does not disrupt activity, or fluorescently labeled tubulin plus vinca alkaloids should provide this information.

Lipophilicity and Cytotoxicity. Drug availability at the tissue level is in part determined by lipophilicity. For drugs that are active intracellularly, more lipophilic drugs should have a greater potential for crossing lipid-rich cell membranes and interacting with their target. For the test compounds examined in this study, there is only a correlation between calculated partition coefficients and L1210 cell cytotoxicity; however, the more cytotoxic compounds tend to be more water-soluble. The measured partition coefficients do not correlate with cytotoxicity. The work of Owellen and co-workers indicated that, for a different set of vinca alkaloids, partition coefficients and drug affinity were important contributors to cytotoxicity in cell culture and in vivo (*10*). Their drug affinity measurements are actually in agreement with our results since the apparent affinity measured in their binding assay is linked to spiral formation and reflects both K_1 and K_2 effects. Their partition coefficient results also agree with our observation that calculated partition coefficients correlate with cytotoxicity. Their studies of 11 vincas included both measured (six compounds) and calculated (five compounds) partition coefficients. The calculated values were determined by using measured values and adding or subtracting estimated values for chemical structure differences. The correlation Owellen et al. (*10*) report is based upon a fit of the cytotoxicity data (log LD_{50}) to a quadratic equation involving log K_{app} + log P + log P^2. To better compare their results with ours, we plotted and linearly fit their log P vs log LD_{50} values in an identical manner to our correlation analysis. The results are similar to our calculated data with $p = 0.08$ and $r = 0.55$ (data not shown). (Note by our criteria these data do not correlate.) There are two drugs in common between our study and theirs. Our measured and calculated log partition coefficients for vinblastine (1.89 and 5.4), and vincristine (1.16 and 4.1) differ from those reported by Owellen and co-workers, as 3.65 and 2.57 for vinblastine and vincristine, respectively, although the relative differences between these two drugs are similar. We can possibly ascribe the difference in our measured values and the Owellen values to differences in aqueous buffer conditions. As discussed in methods, it is possible these compounds lie outside the optimal prediction space for the software we used, and thus the calculated values differ due to bias in the basis set. Nonetheless, we must remain cautious about concluding that partition coefficients are significant predictors of cytotoxicity. As is evident in Figure 4, panel B, the calculated data and the data from Owellen et al. (*10*) suggest cytotoxicity is improved by decreased lipophilicity and increased aqueous solubility. This is not entirely consistent with the simple interpretation presented above that more lipophilic drugs should have a greater potential for crossing lipid-rich cell membranes and interacting with their target. There are two potential factors to explain this discrepancy. First, increased lipophilicity partitions more drug in the membrane phase rather than crossing the cell membrane, thus requiring higher drug concentrations to raise the cytoskeleton concentration. Second, a higher aqueous solubility increases drug concentration at the site of action, the ends of microtubules in the cytoskeleton. Sufficient lipophilicity allows delivery of drug without impeding activity. Undoubtedly other factors are involved.

Microtubule Inhibition and Cytotoxicity. The ability of vinca alkaloids to inhibit microtubule polymerization does not correlate with L1210 cell cytotoxcity (Figure 5). The IC_{50} values range over 3 orders of magnitude, 16 to >1000 nM; however, there is less than a 3-fold difference in IC_{50} values for microtubule inhibition. In fact 10 of the compounds differ by less than 2-fold in their ability to inhibit microtubule polymerization (Table 1). In other words, it is difficult to differentiate these compounds based on their ability to diminish microtubule polymerization (*28*). Furthermore, there is no correlation between tubulin spiral size and microtubule inhibition (Figure 6). Larger or smaller vinca-induced tubulin spirals appear to have similar potential for inhibiting microtubule formation. We conclude that microtubule inhibition is not a predictor of cell culture cytotoxicity, and thus, while turbidity studies identify potential antimitotics (*31*), they have limited translational clinical value.

This result may appear somewhat surprising though, because others have observed a correlation between cytotoxicity and inhibition of MTP polymerization (*11*, *12*) using similar turbidity techniques. (As discussed above, this correlation may be due to the set of drugs analyzed.) The turbidity method measures the amount of drug required to reduce the polymer mass to 50% and assumes turbidity is constant per milligram of protein assembled. If drug induces significant alterations in polymer shape, for example, giving rise to an increase in turbidity per milligram, then the method

might overestimate the IC_{50} value. Borman and co-workers observed numerous altered polymer shapes by EM with MTP and high concentrations of drug. However, at the micromolar and submicromolar IC_{50} concentrations we observed for MTP and PC-tubulin, there are few aberrant microtubule structures in solution. Kruczynski and co-workers reported alterations in cellular microtubules after drug exposure and observed a concentration-dependent dissolution of microtubules followed by formation of paracrystals (*21*). Of relevance to our studies, they observed the same effect with each vinca alkaloid, vincristine, vinblastine, vinorelbine, and vinflunine, but the concentration range shifted proportional to the relative affinity of each drug for tubulin (measured in a competitive binding assay) and relative to the spiraling potential of each drug (measured in a subsequent study by sedimentation methods; ref *8*). Intracellular paracrystals were found at 50 μM vinflunine and at vinorelbine and vinblastine concentrations 3- and 17-fold lower, demonstrating that significant spiral formation is occurring over the range of drug concentrations used in our studies. It is possible that the cellular milieu or cellular factors make the microtubules more dynamic, less stable, and more discriminating to the action of these drugs. It may be even more relevant that Jordan and Wilson have shown the ability to cause mitotic arrest does not require disassembly of cellular microtubules but rather the suppression of microtubule dynamics (*3*, *4*). Thus, techniques that measure the ability of drugs to cause 50% polymer disassembly are measuring features that may be mechanistically irrelevant to the cellular mode of action of the drug, and the observed correlation between spiraling potential and cytotoxicity (Figure 3) most likely indicates that the lifetime of cellular retention is a measure of effects on microtubule dynamics.

Recent work from the laboratory of Jordan and Wilson (*32*, *33*) suggest that vinflunine and vinorelbine disrupt microtubule dynamics by a novel mechanism compared to that of vinblastine. In contrast to vinblastine, vinflunine, and vinorelbine affect neither the rate of microtubule shortening nor the time spent in a pause state. They do slow microtubule growth rates, reduce the shortening duration, and increase the growth duration. A possible difficulty with these studies is that they were done at a single drug concentration, 400 nM. Thus, the observations may reflect differences in the degree of saturation rather than a novel mode of action. Nonetheless, it is possible that different drugs exhibit diverse cellular effects because of differences in their intrinsic affinity for tubulin, spiral polymers, and microtubule ends. More importantly, changes in spiraling potential may translate to differential disruption of dynamics regulation, much of which also occurs at the ends of microtubules (*34*). In addition to direct binding to mitotic spindles, vinca alkaloids may interact, directly or indirectly, with MAPs and/or other regulators of microtubule dynamics such as XKCM1 or OP18. Interactions with these other targets, currently under investigation in our laboratory, may contribute to in vivo vinca alkaloid cytotoxicity and differential effects on tissues.

ACKNOWLEDGMENT

We thank Jeff Ingram for technical assistance with this project. We are grateful to the University of Mississippi Medical Center Analytical Ultracentrifuge Facility. This is UMMC AUF publication 0022. We also thank Pelahatchie Country Meat Packers for providing pig heads for tubulin purification.

REFERENCES

1. Calabresi, P., and Chabner, B. A. (1996) in *Goodman and Gilman The Pharmacological Basis of Therapeutics.* (Hardman, J. G., Limbird, L. E., Molinoff, P. B., Ruddor, R. W, and Goodman Gilman, A., Eds), pp 1209−1263, McGraw-Hill, New York.
2. Johnson, S. A., Harper, P., Hourobagyi, G. N., and Pouillar, V. P. (1996) *Cancer Treat. Rep. 22*, 127−142.
3. Toso, R. J., Jordan, M. A., Farrell, K. W., Matsumoto, B., and Wilson, L. (1993) *Biochemistry 32*, 1285−1293.
4. Jordan, M. A., Thrower, D., and Wilson, L. (1991) *Cancer Res. 51*, 2212−2222.
5. Na, G. C., and Timasheff, S. N. (1980) *Biochemistry 19*, 1355−1365.
6. Lobert, S., and Correia, J. J. (2000) *Methods Enzymol. 323*, 77−103.
7. Lobert, S., Vulevic B., and Correia, J. J. (1996) *Biochemistry 35*, 6806−6814.
8. Lobert, S., Ingram, J. W., Hill, B. T., and Correia, J. J. (1998) *Mol. Pharmacol. 53*, 908−915.
9. Rahmani, R., Gueritte, F., Martin, M., Just, S., Cano, J. P., and Barbet, J. (1986) *Cancer Chemother. Pharmacol. 16*, 223−228.
10. Owellen, R. J., Donigian, D. W., Hartke, C. A., and Hains, F. O. (1977) *Biochem. Pharm. 26*, 1213−1219.
11. Borman, L. S., Kuehne, M. E., Matson, P. A., Marko, I., and Zebovitz, T. C. (1988) *J. Biol. Chem. 263*, 6945−6948.
12. Borman, L. S., and Kuehne, M. E. (1989) *Biochem. Pharm. 38*, 715−724.
13. Fahy, J., Duflos, A., Ribet, J. P., Jacquesy, J. C., Berrier, C., Jouannetaud, M. P., and Zunino, F. (1997) *J. Am. Chem. Soc. 119*, 8576−8577.
14. Jacquesy, J. C., and Fahy, J. (2000) in *Biomedical Chemistry: Applying Chemical Principles to the Understanding and Treatment of Disease* (Torrence, P. F., Ed.), pp 227−246, John Wiley, New York.
15. Williams, R. C., Jr., and Lee, J. C. (1982) *Methods Enzymol. 85*, 376−408.
16. Correia, J. J., Baty, L. T., and Williams, R. C., Jr. (1987) *J. Biol. Chem. 262*, 17278−17284.
17. Detrich, H. W., and Williams, R. C., Jr. (1978) *Biochemistry 17*, 3900−3907.
18. Lobert, S., Frankfurter, A., and Correia, J. J. (1995) *Biochemistry 34*, 8050−8060.
19. Correia, J. J. (2000) *Methods in Enzymology, Numerical Computer Methods, Part C 321*, 81−100.
20. Sangrajrang, S., Zidane, M., Berda, P., More, M. T., Calvo, F., and Fellous, A. (2000) *Cancer Chemother. Pharmacol. 45*, 120−126.
21. Kruczynski, A., Barret, J. M., Etievant, C., Colpaert, F., Fahy, J., and Hill, B. T. (1998) *Biochem. Pharmacol. 55*, 635−648.
22. Leo, A. J. (1987) *J. Pharm Sci. 76*, 166−168.
23. Gombar, V., and Ensloin, K. (1996) *J. Chem. Inf. Comput. Sci. 36*, 1127−1134.
24. Lee, J. C., Harrison, D., and Timasheff, S. N. (1975) *J. Biol. Chem. 250*, 9276−9282.
25. Prakash, V., and Timasheff, S. N. (1983) *J. Biol. Chem. 258*, 1689−1697.
26. Prakash, V., and Timasheff, S. N. (1991) *Biochemistry 30*, 873−880.
27. Muller, W., and Crothers, D. M. (1968) *J. Mol. Biol. 35*, 251−290.
28. Jean-Decoster, C., Brichese, L., Barret, J.-M., Tollon, Y., Kruczynski, A., Hill, B. T., and Wright, M. (1999) *Anti-Cancer Drugs 10*, 537−543.
29. DiCera, E. (1995) *Thermodynamic Theory of Site-Specific Binding Processes in Biological Macromolecules*, Cambridge University Press, New York.
30. Lobert, S., Boyd, C. A., and Correia, J. J. (1997) *Biophys. J. 72*, 416−427.

31. Lobert, S., Ingram, J. W., and Correia, J. J. (1999) *Cancer Res. 59*, 4816−4822.
32. Ngan, V. K., Bellman, K., Panda, D., Jordan, M. A., Wilson, L., and Hill, B. T. (1999) *Proc. Am. Assoc. Cancer Res. 40*, 286.
33. Ngan, V. K., Bellman, K., Panda, D., Hill, B. T., Jordan, M. A., and Wilson, L. (2000) *Cancer Res.*, in press.
34. Walczak, C. E. (2000) *Curr. Opin. Cell Biol. 12*, 52−56.

BI001038R